# Max-Planck-Institut
## für Mathematik
## in den Naturwissenschaften
## Leipzig


**Numerical simulation of generalized KP type equations with small dispersion**

by


*Christian Klein, and Christof Sparber*



Preprint no.: 20 2006


# NUMERICAL SIMULATION OF GENERALIZED KP TYPE EQUATIONS WITH SMALL DISPERSION

CHRISTIAN KLEIN AND CHRISTOF SPARBER

ABSTRACT. We numerically study nonlinear dispersive wave equations of generalized Kadomtsev-Petviashvili type in the regime of small dispersion. To this end we include general power-law nonlinearities with different signs. A particular focus is on the Korteweg-de Vries sector of the corresponding solutions.

version: February 13, 2006

## 1. INTRODUCTION

One of the most important models for nonlinear dispersive waves is the $1+1$ dimensional *Korteweg-de Vries equation* (KdV)

$$\partial_t u + 6u\,\partial_x u + \epsilon^2 \partial_{xxx} u = 0, \tag{1.1}$$

describing shallow water waves, which essentially propagate in only one dimension, *cf.* [10, 22] for further details. In (1.1) we already introduced a scaling suitable for the so-called *small dispersion limit* where $\epsilon \ll 1$. To this end one starts from the unscaled (dimensionless) KdV model

$$\partial_T u + 6u\,\partial_X u + \partial_{XXX} u = 0, \tag{1.2}$$

where $(T, X)$ are now considered as the natural length scales in this problem. Introducing slowly varying solutions of the form $u = u(\epsilon T, \epsilon X)$, $0 < \epsilon \ll 1$, plugging them into (1.2) and denoting $(t, x) = (\epsilon T, \epsilon X)$, we obtain the scaled equation (1.1). Thus, in all what follows the notion of the coordinates refers to the slow scales $t, x$.

In order to take into account also (weak) transverse effects in the propagation of shallow water waves, a natural generalization of the KdV equation is the $2+1$ dimensional *Kadomtsev-Petviashvili equation* (KP)

$$\partial_x\big(\partial_t u + 6u\,\partial_x u + \epsilon^2 \partial_{xxx} u\big) + \lambda\,\partial_{yy} u = 0, \quad \lambda = \pm 1, \tag{1.3}$$

see, *e.g.*, [10, 11] for a physical derivation. The case $\lambda = -1$ corresponds to the so-called KP-I model, valid for strong surface tension, whereas $\lambda = +1$ is usually referred to as KP-II equation, used in the case of weak surface tension. Clearly, any $y$-independent solution of (1.3) is a solution of (1.1), forming the so-called *KdV sector*. Both, the KdV and the KP equation, are known to be *completely integrable*, thus comprising an infinite number of conservation laws [1]. Moreover, explicit solutions for both of them can be obtained via the *inverse scattering* method [2, 19].

2000 *Mathematics Subject Classification.* 35Q53, 74S25, 34E15.

*Key words and phrases.* (modified) Korteweg-de Vries equation, Kadomtsev-Petviashvili equation, nonlinear dispersive models, modulation theory.

This work has been supported by the APART research grant of C.S. funded by the Austrian Academy of Sciences.

In this work we shall consider the following *generalization* of the KP equation (gKP)

$$\partial_x\big(\partial_t u + 6\sigma u^n\,\partial_x u + \epsilon^2\partial_{xxx}u\big) + \lambda\,\partial_{yy}u = 0, \quad \sigma = \pm 1, \tag{1.4}$$

where $n \in \mathbb{N}$ allows for higher order nonlinearities as studied in, *e.g.*, [6]. Thus, if we consider $y$-independent solutions of (1.4) we get a generalized KdV type model (gKdV) of the following form,

$$\partial_t u + 6\sigma u^n\,\partial_x u + \epsilon^2\partial_{xxx} = 0. \tag{1.5}$$

For $n = 2$ and $\sigma = \pm 1$, equation (1.5) furnishes the focussing resp. defocussing *modified* KdV equation [21]. Note however, that the case $n = 2$ for (1.4) does *not* yield the *modified KP equation*, which carries a further nonlinear term and can be obtained as a higher order equation within the so-called KP hierarchy [14].

In what follows we shall study (1.4) in its *evolutionary form*, *i.e.*

$$\begin{cases} \partial_t u + 6\sigma u^n\,\partial_x u + \epsilon^2\partial_{xxx}u + \lambda\,\partial_x^{-1}\partial_{yy}u = 0, \\ u\big|_{t=0} = \phi(x,y), \end{cases} \tag{1.6}$$

where the anti-derivative $\partial_x^{-1}$ is defined as a *Fourier multiplier* with the singular symbol $-\mathrm{i}/k_x$ (see [4, 7, 18] for several mathematical results on (1.6) with $n = 1$).

In this work we shall be interested in a numerical study of solutions to (1.4), and their corresponding KdV sector, in the regime $\epsilon \ll 1$. In particular we are interested in the influence of the considered higher order nonlinearities and their respective signs. For the classical KdV equation (1.1), the limit $\epsilon \to 0$ has attracted lots of interest in various branches of mathematics. Obviously this is a highly *singular* limiting regime which requires particular care. Nowadays, a rigorous asymptotic treatment of this problem has been established for the cases $n = 1$ (classical KdV) and $n = 2$ (modified KdV), *cf.* [9, 16, 17, 20] and the references given therein. The quoted results heavily rely on inverse scattering techniques and complete integrability, which in particular implies that the case $n > 2$ is still open. Let us also refer to [8, 12] for numerical studies of such problems.

On the other hand, an analogous comprehensive treatment for KP type models is an unsolved mathematical problem so far. To our knowledge, the only rigorous results in this direction are currently available in [3, 15]. To shed some light on these questions a numerical study of the small dispersion KP equation has been recently given by the authors in [13]. The present paper can be seen as a continuation of this earlier work, taking into account higher order nonlinearities. We hope that our studies allow for further insight in the role of dispersion in nonlinear wave equations.

## 2. Remarks on the dispersionless limits

The formal limit, as $\epsilon \to 0$, of (1.6) yields the *dispersionless* gKP equation

$$\begin{cases} \partial_t u + 6\sigma u^n\,\partial_x u + \lambda\,\partial_x^{-1}\partial_{yy}u = 0, \\ u\big|_{t=0} = \phi(x,y). \end{cases} \tag{2.1}$$

However we do not expect this equation to be a correct description of the dispersionless limit for all times. In particular for $y$-independent solutions we find the following (generalized) *Hopf type equation*

$$\partial_t u + 6\sigma u^n\,\partial_x u = 0, \tag{2.2}$$

which is known to provide a reliable approximation of the limiting KdV solution only up to some finite time $t_c \geq 0$. This can be seen by integrating equation (2.2)

(implicitly) via the method of characteristics, *i.e.*

$$u(t,x) = f(\xi), \quad x = \xi + 6\sigma t f^n(\xi), \tag{2.3}$$

for some initial condition $u(0,x) = f(x)$. This construction however only works up to the time

$$t_c = \min_{\xi} \left[ -\frac{\sigma}{6\partial_\xi (f^n(\xi))} \right], \tag{2.4}$$

where the minimum is determined for $\xi$ given by $u(t,x) = f(\xi)$, *i.e.* as the maximum of $|f'(\xi)|$ for negative $f'(\xi)$. For times $t > t_c$, the solution $u(t,x)$, as given by (2.3), becomes multi-valued. Also, at $t = t_c$ the gradient of $u(t,x)$ w.r.t. $x \in \mathbb{R}$ diverges, marking the onset of a shock wave in the corresponding weak solution to (2.2).

For small but still nonzero $\epsilon \ll 1$, it is well known, that solutions of the gKdV equation for $t < t_c$ will behave qualitatively as the corresponding solution to the generalized Hopf equation, the latter being a strong limit of the former as $\epsilon \to 0$. For $t \geq t_c$, however, the solutions to the gKdV equation will develop a zone of rapid modulated oscillations with wavelength of the order $1/\epsilon$. These oscillations consequently smear out the shock fronts visible in the weak solution of (2.2). Moreover the oscillatory zone within the gKdV equation roughly coincides with the region where the corresponding Hopf solution is multi-valued.

As already pointed out in [13] the analogous situation in the KP case is less clear, although our numerical studies show several qualitative similarities. Essentially this is due to the fact that the dispersionless KP equation cannot be integrated by the method of characteristics. Moreover it is not clear how to solve, in an appropriate way, the corresponding *Whitham modulation equations*, which are used in the KdV case to identify the oscillatory zones and to construct the asymptotic solution there. In [13], we established numerically that for $t < t_c$ the KP equation converges to the corresponding dispersionless model with the rate $\sim \mathcal{O}(\epsilon^{3/2})$.

From the numerical point of view we circumvented the problem of shock solutions within the limiting dispersionless model in [13] by using a *dissipative regularization*. More precisely we add to (2.1) a small dissipative term of the form

$$\partial_x(\partial_t u + 6u^n\,\partial_x u - \mu\,\partial_{xx} u) + \lambda\,\partial_{yy} u = 0. \tag{2.5}$$

where $0 < \mu \ll 1$ being some small real-valued parameter, such that $\mu \sim \mathcal{O}(1)$, as $\epsilon \to 0$. Although (2.5) does no longer conserve the mass, *i.e.*

$$M[u(t)] := \int_{\mathbb{R}} \int_{\mathbb{R}} \mathrm{d}x\,\mathrm{d}y\, u^2(t,x,y), \tag{2.6}$$

we still expect that, as $\mu \to 0$, the corresponding regularized solution tends to some kind of entropy solution for the dispersionless equation. More details on the numerical treatment of (1.4) of the considered equations can be found in [13] and in Appendix A below.

## 3. Numerical study of small dispersion regimes

As a concrete example we shall consider the initial data given by

$$\phi_\delta = -\,\partial_x \mathrm{sech}^2(r), \quad r := \sqrt{x^2 + \delta y^2}, \tag{3.1}$$

where $\delta \in [0,1]$ is a small deformation parameter. This choice of $\phi$ consequently allows for a continuous deformation of the KdV sector within the solution of the

gKP model. Note that the initial data are rapidly decreasing as $|x|, |y| \to \infty$. Another reason for our initial condition is that $\phi_\delta$ is subject to the constraint

$$\int_{\mathbb{R}} \mathrm{d}x\, \phi_\delta(x, y) = 0, \quad \forall\, y \in \mathbb{R}, \tag{3.2}$$

which turns out to be a necessary condition for admissible KP initial data, *cf.* [13] for more details on this. In the present paper we will only consider the cases $\delta = 0$ (KdV) and $\delta = 1$. For the discussion of other values of $\delta$, see [13].

3.1. **Generalized Hopf equation with dissipative regularization.** The study of a dissipative regularization of the gKP equation as in (2.5) allows on the one hand to identify regions where shocks form, and on the other hand, to numerically approximate the corresponding entropy solution. We illustrate this concept in the gKdV case. For examples in the KP setting, see again [13].

First, consider the classical quadratic case $n = 1$ and $\sigma = -1$ with the initial data (3.1). As can be seen from Fig. 1, there is only a single shock front which forms roughly for $t = 0.08$. This is different from the situation encountered in, *e.g.*, the

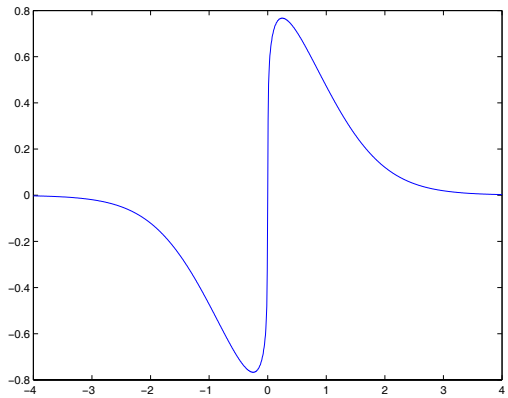


FIGURE 1. Solution to the regularized Hopf equation ($n = 1$) for initial data (3.1), $\mu = 0.01$ and $\sigma = -1$ at time $t = 0.09$.

cubic case where $n = 2$ and $\sigma = 1$, as it is shown in Fig. 2. A first (regularized) shock appears for $t \approx 0.1$ in the region of negative initial data. The width of the shock front is of the order $1/\mu$ where we have chosen $\mu = 0.01$. However, for $t \approx 0.22$, a second shock front appears in the region of positive initial data. Due to the dispersive regularization for small but non-zero $\epsilon$, rapid oscillations are expected to smooth out these shocks. As was shown in [8], these oscillations always appear for finite $\epsilon$ shortly before the time $t_c$ is reached. Consequently we expect only a single oscillatory zone in the classical (quadratic) KdV setting to be discussed below.

3.2. **gKdV equation with small dispersion.** Let us now focus on the KdV sector, *i.e.* $\delta = 0$ in (3.1), choosing $\epsilon = 0.1$. We show the corresponding solution to the classical KdV equation, *i.e.* $n = \sigma = 1$, for several values of $t$ in Fig. 3. It can be seen that the first oscillations form at $t \approx 0.18$. In this example the oscillations are more pronounced in the region of negative initial data. The analogous situation is shown for $n = 1$ but $\sigma = -1$ in Fig. 4. In this case the oscillations start much earlier, roughly at time $t \approx 0.06$. As expected there is only one oscillatory zone

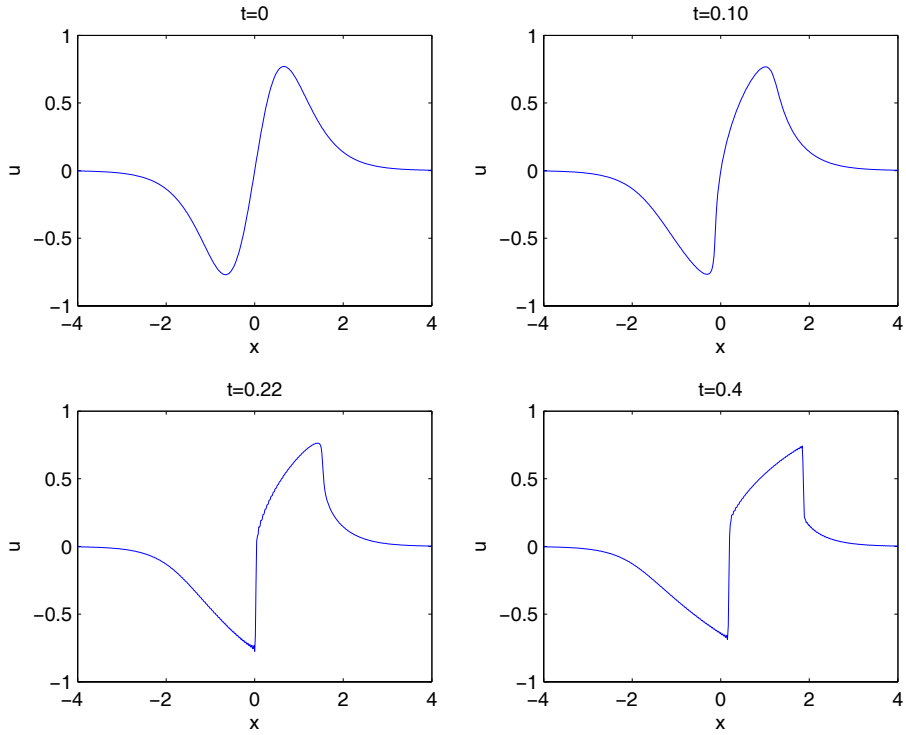


FIGURE 2. Solution to the regularized generalized Hopf equation for several values of $t$, as obtained from the initial data (3.1), with $\mu = 0.01$, $n = 2$, and $\sigma = 1$.

which is located between the extrema of the initial data. The oscillations are similar to those for negative initial data in the case $\sigma = 1$, but much more pronounced.

In the case $n = 2$ and $\sigma = 1$ (again $\epsilon = 0.1$) the corresponding solution can be seen in Fig. 5. Here, the oscillations appear much earlier than in the classical case above. Indeed, the first oscillation is clearly visible at $t \approx 0.08$. Again the oscillations are more pronounced in the region of negative initial data. For $\sigma = -1$, the corresponding situation is given in Fig. 6. This time however, the oscillations start later, roughly at time $t \approx 0.12$. The oscillations in the region of negative initial data are similar to those in the case $\sigma = 1$. In contrast to the case $n = 1$, $\sigma = -1$, there are two oscillatory regions in this example. The plots for the above solutions at time $t = 0.4$ are presented in one frame in Fig. 7.

For higher nonlinearities, the situation is qualitatively the same. For example, in the case $n = 3$, $\sigma = 1$, as shown in Fig. 8 for $t = 0.4$, the oscillations are similar to the ones in the case $n = 1$, $\sigma = 1$, *cf.* Fig. 3, but they are smaller in amplitude. Note that the almost linear part of the solution, appearing between the oscillatory regions in the KdV case, is strongly deformed in the present example. Finally, the solution for $n = 4$ and $\sigma = 1$ at time $t = 0.4$ is shown in Fig. 9. Again, the situation is qualitatively similar to the case $n = 2$, $\sigma = 1$ in Fig. 5, but there a fewer oscillations. Thus the higher nonlinearity seems to suppress oscillations in both examples.

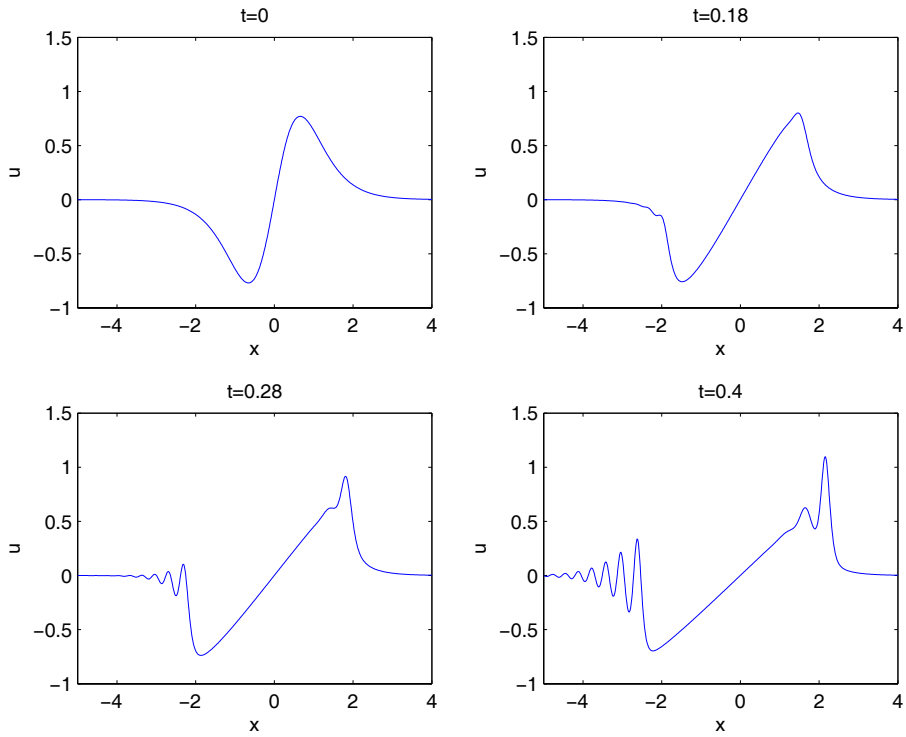


FIGURE 3. Solution to the KdV equation for initial data (3.1) and $\epsilon = 0.1$, $\sigma = 1$ for several values of $t$.

3.3. **gKP equation with small dispersion.** In this section we will study solutions to the generalized KP equations for the initial data (3.1). We will restrict ourselves to the case $\lambda = -1$ and $\epsilon = 0.1$, *i.e.* the generalized KP-I equation in the limit of small dispersion.

The solution for the classical KP-I equation (*i.e.* for $n = 1$ and $\sigma = 1$) at time $t = 0.4$ was already presented in [13]. It it shown Fig. 10. Note that tails towards $x \to \infty$ have formed. The oscillations close to these tails are enhanced in comparison to the KdV case. On the other hand, the oscillations for negative $x$ are weaker than in the KdV case. In [13], this led us to the conclusion that the mass which is transferred to the KP tails leads to stronger gradients within the corresponding dKP equation and thus to stronger oscillations in the KP-I equation. The same situation for $\sigma = -1$ can be seen in Fig. 11. As in the KdV case, there are only oscillations in the region corresponding to negative initial data. In the case $n = 2$ and $\sigma = 1$, the corresponding solution can be seen in Fig. 12. Again the oscillations are enhanced on the side, where the tails appear, as is more visible from the solution on the $x$-axis in Fig. 14.

As can be seen in Fig. 13, there are no oscillations on the side of the tails in the case $n = 2$ and $\sigma = -1$, but the tails are very strong. The relation to the gKdV case is more obvious from Fig. 14 from which it can be inferred that the oscillations on the opposing side of the tails are weakened.

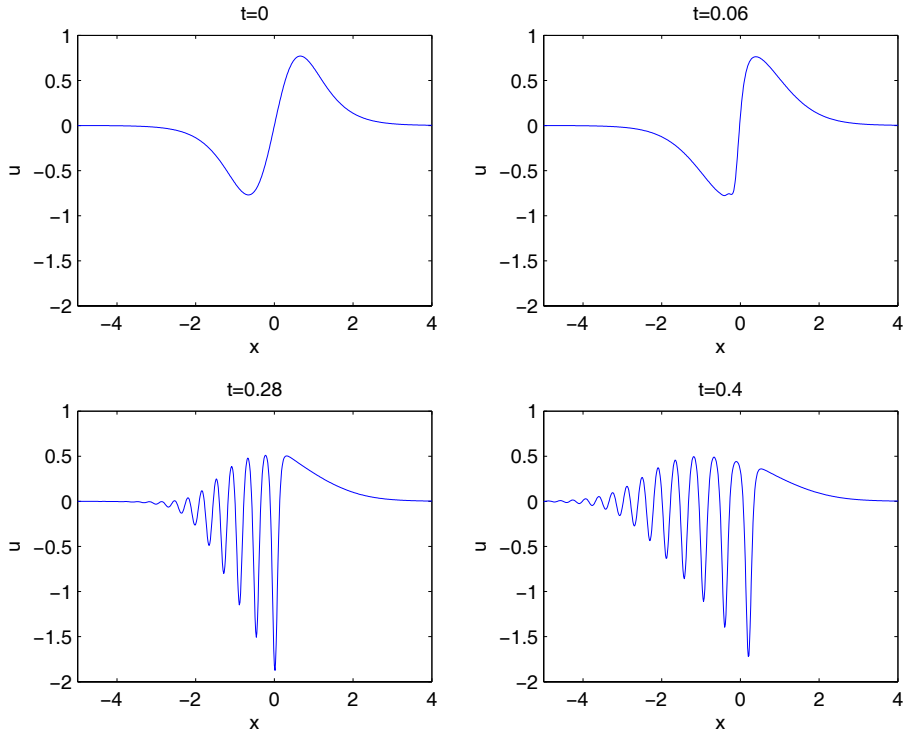


FIGURE 4. Solution to the gKdV equation with $n = 1$ and $\sigma = -1$ for initial data (3.1) and $\epsilon = 0.1$ for several values of $t$.

We show the above presented solutions on the $x$-axis in Fig. 14 where it can be compared directly with Fig. 7 for the corresponding KdV solutions. A qualitative similarity is obvious, as are the differences which mainly show that the gradients and thus the oscillations are enhanced in the vicinity of the tails.

The same tendency can also be observed for higher nonlinearities. In Fig. 15 we show the case $n = 3$, $\sigma = 1$ at $t = 0.4$. With respect to the corresponding gKdV case in Fig. 8, the oscillations near the tails are enhanced, whereas those on the opposing side are weakened. This is even more obvious from Fig. 16 where the potential is shown on the $x$-axis. The same holds true for the case $n = 4$, $\sigma = 1$ as can be seen from Fig. 17 and Fig. 9. The corresponding solution on the $x$-axis is shown in Fig. 18.

## APPENDIX A. THE NUMERICAL METHOD

In this paper we discuss numerical solutions to initial value problems to the generalized KP equation (1.6). We are interested in initial data which decay rapidly as $|x|, |y| \to \infty$ (for example Schwartz functions). This allows for the use of Fourier spectral methods for the spatial coordinates. Thus we treat the problem in a periodic setting w.r.t. $x$ and $y$ with periods $2\pi/L_x$ and $2\pi/L_y$, respectively. It is known that for such initial data the KP solution will develop tails which decay only algebraically in both spatial coordinates, as can be already seen from the Green's function of the linearized model, *cf.* [13]. These tails consequently lead

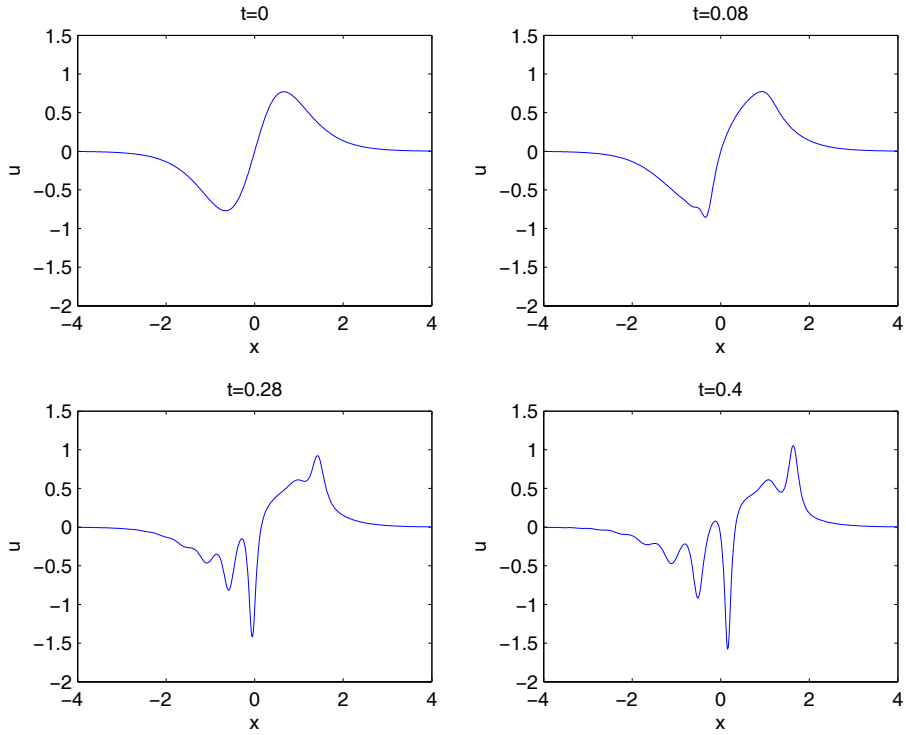


FIGURE 5. Solution to the gKdV equation with $n = 2$ and $\sigma = 1$ for initial data (3.1) and $\epsilon = 0.1$ for several values of $t$.

to a discontinuity of the solution at the boundaries of the domain which yields a Gibbs phenomenon. In addition, the periodicity condition implies the existence of "echoes" for these tails. However, as discussed in more detail in [13], we can choose the domain via $L_x$ and $L_y$ large enough such that neither the Gibbs phenomenon due to the tails nor the echoes influence the oscillatory regions we are interested in. The accuracy of the code will be controlled by the conservation of the mass (2.6), a feature which is not implemented directly in the code. Thus mass conservation presents a strong test for the accuracy of our method.

We denote by

$$\widehat{u}(t,k_x,k_y) := \int_{\mathbb{R}^2} u(t,x,y)\,\mathrm{e}^{-\mathrm{i}(k_x x+k_y y)}\,\mathrm{d}x\,\mathrm{d}y,$$

the *Fourier transform* of $u(t)$ w.r.t. $x$ and $y$, and by $\widehat{u^{n+1}}$ the Fourier transform of $u^{n+1}$. Then we get from equation (1.6)

$$\partial_t \widehat{u} + \frac{\mathrm{i}6k_x\sigma}{n+1}\,\widehat{u^{n+1}} - \epsilon^2\mathrm{i}k_x^3\,\widehat{u} + \mathrm{i}\lambda\frac{k_y^2}{k_x}\,\widehat{u} = 0. \tag{A.1}$$

This is equivalent to

$$\partial_t\left(\exp\left(\mathrm{i}(k_y^2/k_x - \epsilon^2\mathrm{i}k_x^3)t\right)\widehat{u}\right) + \exp\left(\mathrm{i}(k_y^2/k_x - \epsilon^2\mathrm{i}k_x^3)t\right)\frac{\mathrm{i}6k_x\sigma}{n+1}\,\widehat{u^{n+1}} = 0. \tag{A.2}$$

The use of an integrating factor elliminates a stiff part in the equations and allows for the use of explicit schemes with larger time steps. In the present work, we

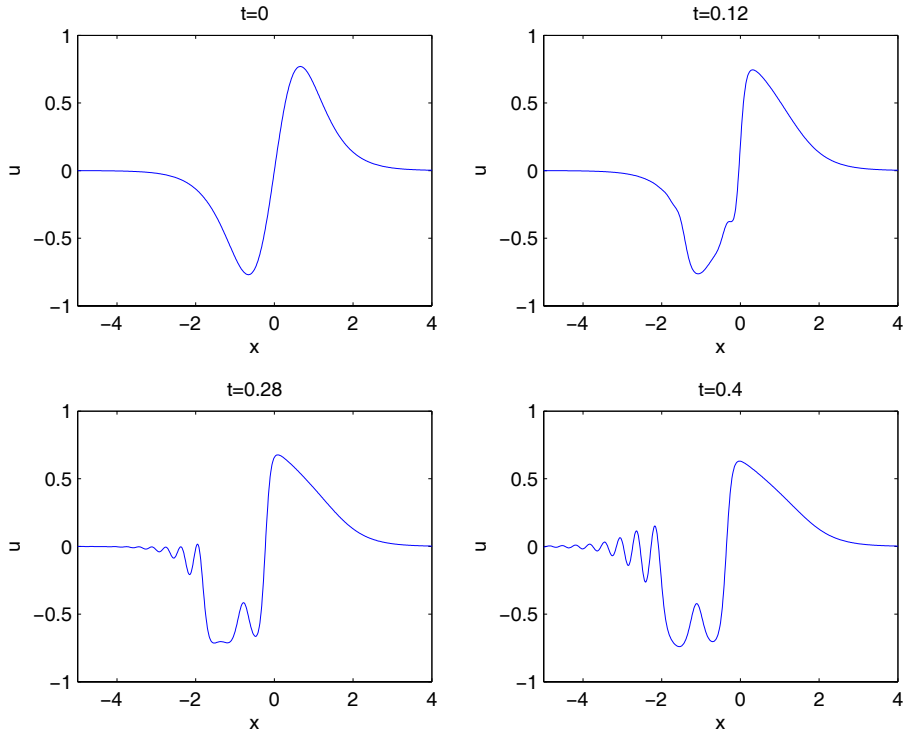


FIGURE 6. Solution to the gKdV equation with $n = 2$ and $\sigma = -1$ for initial data (3.1) and $\epsilon = 0.1$ for several values of $t$.

use a fourth order Runge–Kutta method. The code is stable for time steps of the order $\Delta t = 10^{-4}$ with 2048 modes in the gKdV examples, and $\Delta t = 8 \times 10^{-5}$ with $N_x = 2048$, $N_y = 128$ modes ($L_x = L_y = 5$). With these values we achieve relative mass conservation better than $10^{-4}$ for the gKP computations and better than $10^{-8}$ in the gKdV cases.

## REFERENCES

1. M. J. Ablowitz and P. A. Clarkson, *Solitons, nonlinear evolution equations and inverse scattering*, Cambridge Univ. Press, Cambridge (1991).
2. J. C. Alexander, R. L. Pego, and R. L. Sachs, *On the transverse instability of solitary waves in the Kadomtsev-Petviashvili equation*, Phys. Lett. A **226** (1997), 187–192.
3. V. N. Bogaevskiĭ, *On Korteweg-de Vries, Kadomtsev-Petviashvili, and Boussinesq equations in the theory of modulations*, Zh. Vychisl. Mat. i Mat. Fiz. **30** (1990), no. 10, 1487–1501; translation in U.S.S.R. Comput. Math. and Math. Phys. **30** (1991), no. 5, 148–159.
4. M. Boiti, F. Pempinelli, and A. Pogrebkov, *Properties of solutions of the Kadomtsev-Petviashvili I equation*, J. Math. Phys. **35** (1994), issue 9, 4683–4718.
5. A. de Bouard and Y. Martel, *Nonexistence of $L^2$-compact solutions of the Kadomtsev-Petviashvili II equation*, Math. Annalen. **328** (2004), 525–544.
6. A. de Bouard and J. C. Saut, *Symmetries and decay of the generalized Kadomtsev-Petviashvili solitary waves*, SIAM J. Math. Anal. **28** (1997), no. 5, 1064–1085.
7. J. Bourgain, *On the Cauchy problem for the Kadomtsev-Petviashvili equation*, Geom. Funct. Anal. **3** (1993), no.4, 315–341.
8. T. Grava and C. Klein, *Numerical solution of the small dispersion limit of Korteweg de Vries and Whitham equations*, preprint, arXiv: `math-ph/0511011`.

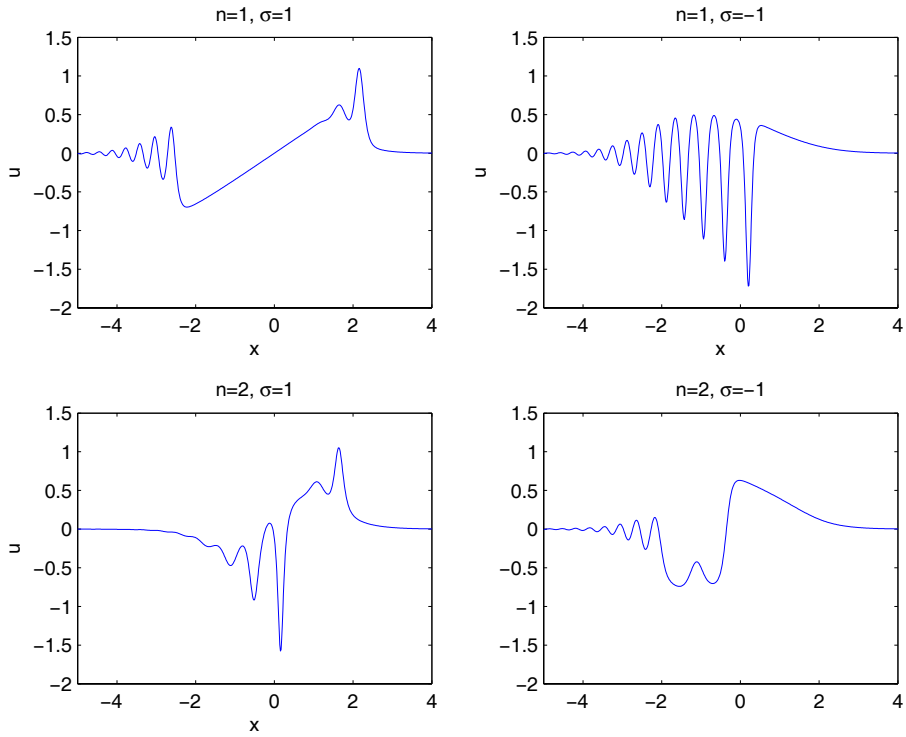


FIGURE 7. Solution to the gKdV equations for initial data (3.1) and $\epsilon = 0.1$ at time $t = 0.4$ for several values of $n$ and $\sigma$.

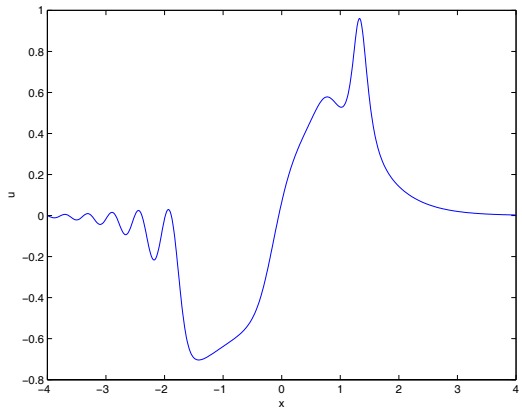


FIGURE 8. Solution to the gKdV equation for initial data (3.1) and $\epsilon = 0.1$, $n = 3$ and $\sigma = 1$ at time $t = 0.4$.

9. T. Grava and Fei-Ran Tian, *The generation, propagation, and extinction of multiphases in the KdV zero-dispersion limit*, Comm. Pure Appl. Math. **55** (2002), no. 12, 1569–1639.
10. R. S. Johnson, *The classical problem of water waves: a reservoir of integrable and nearly integrable equations*, J. Nonl. Math. Phys. **10** (2003) 72–92.

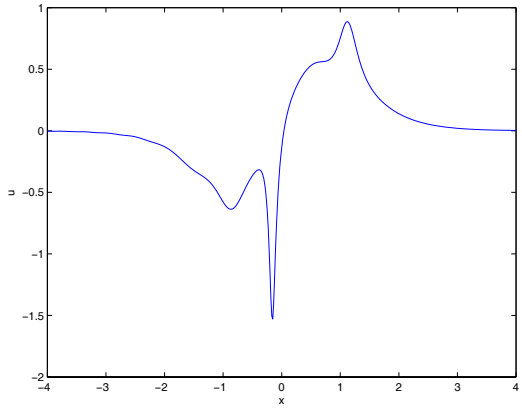


FIGURE 9. Solution to the gKdV equation for initial data (3.1) and $\epsilon = 0.1$, $n = 4$ and $\sigma = 1$ at time $t = 0.4$.

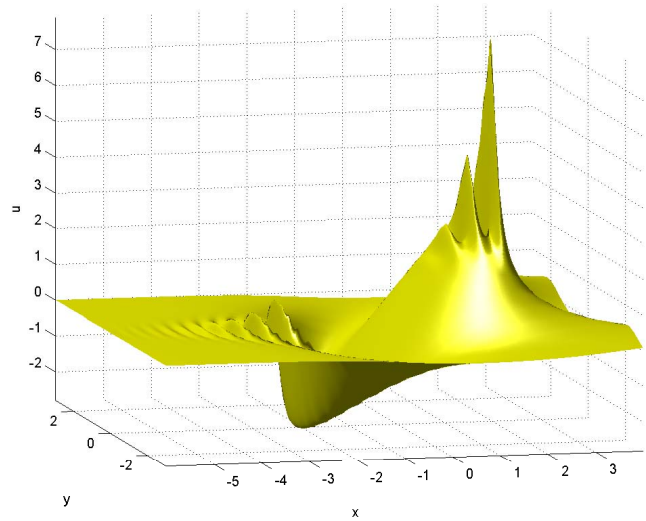


FIGURE 10. Solution to the gKP-I equation with $n = 1$ and $\sigma = 1$ at $t = 0.4$, for initial data (3.1) and $\epsilon = 0.1$.

11. B. B. Kadomtsev and V. I. Petviashvili, *On the stability of solitary waves in weakly dispersing media*, Sov. Phys. Dokl. **15** (1970), 539–541.
12. A. M. Kamchatnov, A. Spire, and V. V. Konotop, *On dissipationless shock waves in a discrete nonlinear Schrödinger equation*, J. Phys. A **37** (2004), no. 21, 5547–5568.
13. C. Klein, C. Sparber, and P. Markowich, *Numerical study of oscillatory regimes in the Kadomtsev-Petviashvili equation*, preprint, arXiv: `math-ph/0601025`.
14. B. G. Konopechenko and V. G. Dubrovsky, *Inverse spectral transform for the modified Kadomtsev-Petviashvili equation*, Stud. Appl. Math. **86** (1992), no. 3, 219–268.
15. I. M. Krichever, *The averaging method for two-dimensional integrable equations*, Funktsional. Anal. i Prilozhen. **22** (1988), no. 3, 37–52; translation in Funct. Anal. Appl. **22** (1989), no. 3, 200–213.
16. P. D. Lax and C. D. Levermore, *The small dispersion limit of the Korteweg de Vries equation I,II,III*, Comm. Pure Appl. Math. **36** (1983), 253–290, 571–593, 809–830.

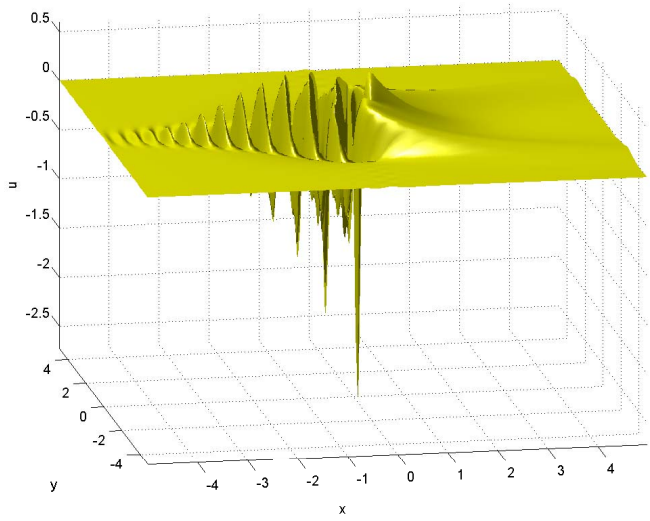


FIGURE 11. Solution to the gKP-I equation with $n = 1$ and $\sigma = -1$ at $t = 0.4$, for initial data (3.1) and $\epsilon = 0.1$.

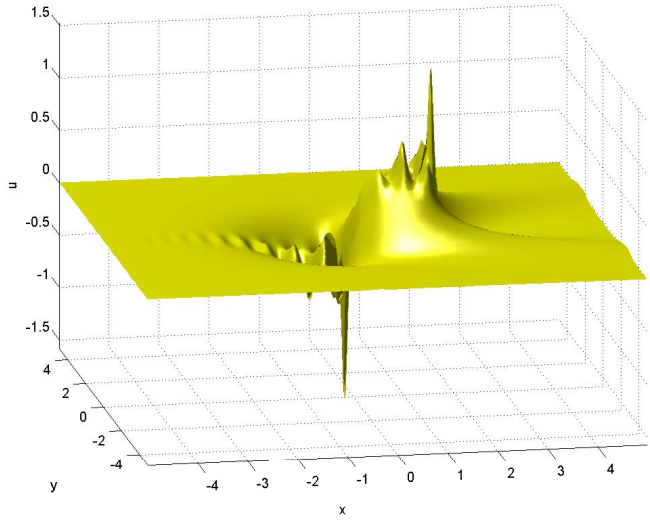


FIGURE 12. Solution to the gKP-I equation with $n = 2$ and $\sigma = 1$ at time $t = 0.4$, for initial data (3.1) and $\epsilon = 0.1$.

17. C. D. Levermore, *The hyperbolic nature of the zero dispersion KdV limit*, Comm. Part. Diff. Equ. **13** (1988), no. 4, 495–514.
18. L. Molinet, J. C. Saut, and N. Tzvetkov, *Well-posedness and ill-posedness results for the Kadomtsev-Petviashvili-I equation* Duke Math. J. **115** (2002), no. 2, 353-384.
19. S. Novikov, S. V. Manakov, L. P. Pitaevskii, and V. E. Zakharov, *Theory of Solitons: The Inverse Scattering Method* Springer Monographs in Contemporary Mathematics, Springer 1984.
20. F. R. Tian, *Oscillations of the zero dispersion limit of the Korteweg de Vries equations*, Comm. Pure App. Math. **46** (1993), 1093–1129.

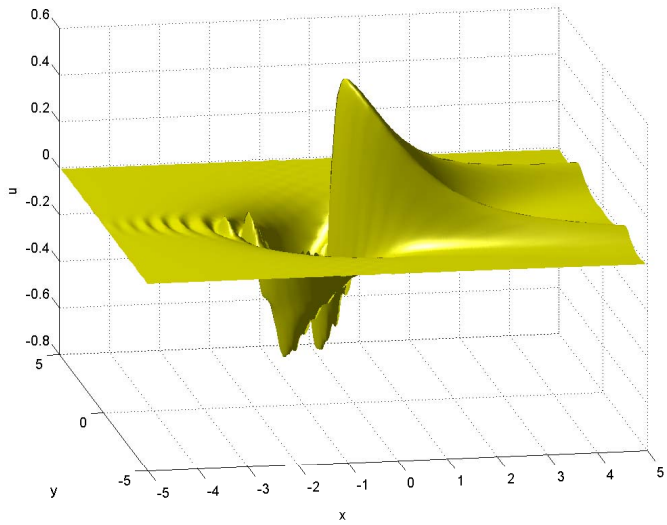


FIGURE 13. Solution to the gKP-I equation with $n = 2$ and $\sigma = -1$ at $t = 0.4$, for initial data (3.1) and $\epsilon = 0.1$.

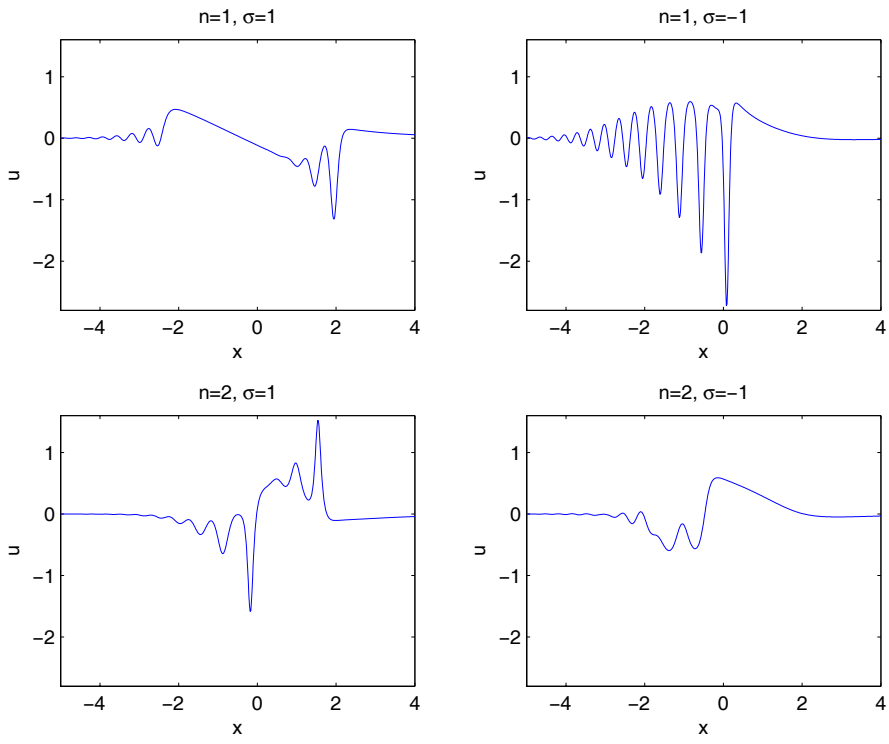


FIGURE 14. Solution to the gKP equations for initial data (3.1) and $\epsilon = 0.1$ at time $t = 0.4$ for several values of $n$ and $\sigma$.

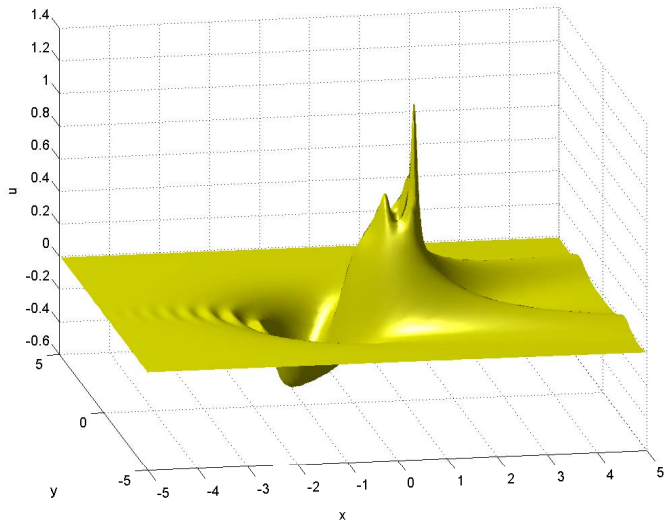


FIGURE 15. Solution to the gKP-I equation with $n = 3$ and $\sigma = 1$ at $t = 0.4$, for initial data (3.1) and $\epsilon = 0.1$.

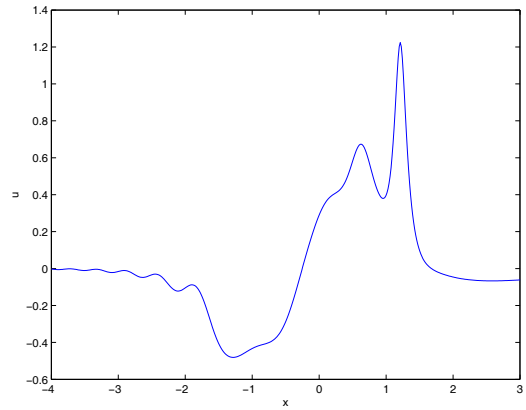


FIGURE 16. Solution to the gKP-I equation with $n = 3$ and $\sigma = 1$ at $t = 0.4$ on the $x$-axis, for initial data (3.1) and $\epsilon = 0.1$.

21. M. Wadati, *The modified Korteweg-de Vries equation*, J. Phys. Soc. Japan **34** (1973), 1289–1296.
22. G. B. Whitham, *Linear and nonlinear waves*, Wiley (1974).

MAX PLANCK INSTITUTE FOR MATHEMATICS IN THE SCIENCES

*E-mail address*: klein@mis.mpg.de

WOLFGANG PAULI INSTITUTE VIENNA & FACULTY OF MATHEMATICS, VIENNA UNIVERSITY, NORDBERGSTRASSE 15, A-1090 VIENNA, AUSTRIA

*E-mail address*: christof.sparber@univie.ac.at

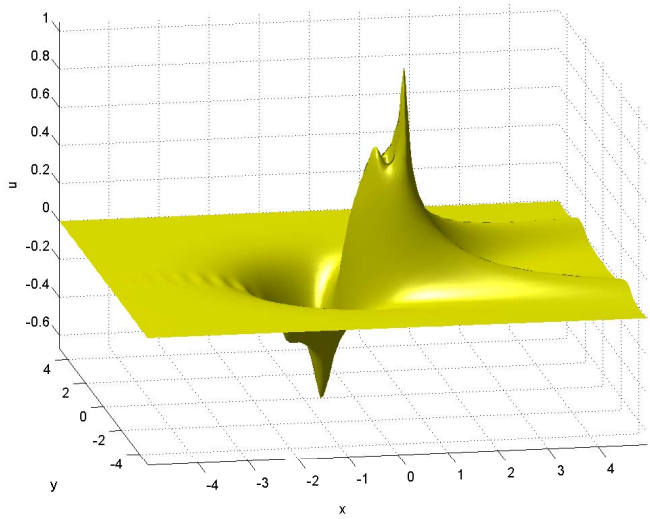


FIGURE 17. Solution to the gKP-I equation with $n = 4$ and $\sigma = 1$ at $t = 0.4$, for initial data (3.1) and $\epsilon = 0.1$.

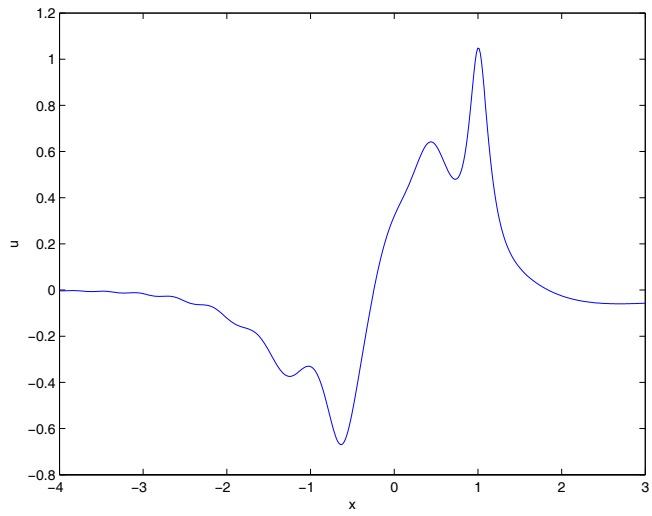


FIGURE 18. Solution to the gKP-I equation with $n = 4$ and $\sigma = 1$ at $t = 0.4$ on the $x$-axis, for initial data (3.1) and $\epsilon = 0.1$.